International Journal of Physical Sciences

ABOUT IJPS

The **International Journal of Physical Sciences (IJPS)** is published weekly (one volume per year) by Academic Journals.

International Journal of Physical Sciences (IJPS) is an open access journal that publishes high-quality solicited and unsolicited articles, in English, in all Physics and chemistry including artificial intelligence, neural processing, nuclear and particle physics, geophysics, physics in medicine and biology, plasma physics, semiconductor science and technology, wireless and optical communications, materials science, energy and fuels, environmental science and technology, combinatorial chemistry, natural products, molecular therapeutics, geochemistry, cement and concrete research, metallurgy, crystallography and computer-aided materials design. All articles published in IJPS are peer-reviewed.

Contact Us

Editorial Office:	ijps@academicjournals.org
Help Desk:	helpdesk@academicjournals.org
Website:	http://www.academicjournals.org/journal/IJPS
Submit manuscript online	http://ms.academicjournals.me/

International Journal of Physical Sciences

Full Length Research Paper

Some classifications on $\alpha-$ Kenmotsu manifolds

Saadet DOĞAN* and Müge KARADAĞ

Department of Mathematics 44069, Faculty of Arts and Science, Inonu University, Malatya/Turkey.

In this paper, we investigate some curvature problems of $\alpha-$ Kenmotsu manifolds satisfying some certain conditions and we reach some classicifications. We consider φ-recurrent $\alpha-$ Kenmotsu manifolds and we show that φ-recurrent $\alpha-$ Kenmotsu manifolds are also η-Einstein manifolds. Next, we study φ-Ricci symmetric $\alpha-$ Kenmotsu manifolds and we find this manifolds are Einstein manifolds too. In addition, we examine locally φ-symmetric α-Kenmotsu manifolds. Later we investigate this type manifold with quasi-conformally curvature tensor and concircular curvature tensor. In addition to these, we construct an example of $\alpha-$ Kenmotsu manifolds and we see that this example is a locally $\varphi-$ symmetric $\alpha-$ Kenmotsu manifold.

Key words: $\alpha-$ Kenmotsu manifold, φ-recurrent, φ-Ricci symmetric, locally φ-symmetric, concircular curvature tensor, quasi-conformally curvature tensor, η-Einstein manifolds, Einstein manifolds.

INTRODUCTION

Janssens and Vanhecke (1981) define $\alpha-$ Kenmotsu manifolds. These are trans-sasakian of type (0, α) in J. A. Oubina's sense (Oubina, 1985). Öztürk et al. (2010) study about $\alpha-$ Kenmotsu manifolds satisfying some curvature conditions. Dileo (2011) write paper named "A classification of certain almost $\alpha-$ Kenmotsu manifolds". On the other hand De (2014) study globally $\varphi-$ quasi-conformally symmetric $\alpha-$ Kenmotsu manifold and give some examples 3-dimensional $\alpha-$ Kenmotsu manifolds. We generally have interest on conditions about curvature tensor, because curvature tensors play important role in geometry and physics. For example; concircular

transformation transforms every geodesic circle of a Riemannian manifold *M* into a geodesic circle. An interesting invariant of a concircular transformation is the concircular curvature tensor (Yano, 1940). In this paper, we study φ-recurrent $\alpha-$ Kenmotsu manifolds. In additon to this, we investigate $\varphi-$ ricci symmetric $\alpha-$ Kenmotsu manifolds and show that $\varphi-$ ricci symmetric $\alpha-$ Kenmotsu manifolds are Einstein manifolds. In differential geometry and mathematical physics, an Einstein manifold is a Riemannian or pseudo-Riemannian manifold whose Ricci tensor is

*Corresponding author. E-mail: saadetdoganmat@gmail.com

proportional to the metric. They are named after Albert Einstein because this condition is equivalent to saying that the metric is a solution of the vacuum Einstein field equations (Besse, 1987). Next, we deal with locally $\varphi - $ symmetric α Kenmotsu manifolds and we prove some theorems about the scalar curvature of the manifolds. In addition to these, we consider quasi-conformally flat condition on this type manifolds. We find interesting results when we investigate concircularly flat condition on locally $\varphi - $ symmetric α -Kenmotsu manifolds.

MATERIALS AND METHODS

Let *(M; g)* be an *(2n + 1)*-dimensional Riemannian manifold. We denote by ∇ the covariant differentiation with respect to the Riemannian metric *g*. The Ricci tensor of *M* are defined by

$$S(X,Y) = \sum_{i=1}^{2n+1} R(e_i, X, Y, e_i) \tag{1}$$

where $\{e_1, e_2, ..., e_{2n+1}\}$ is a locally orthonormal frame and *X, Y* are vector fields on *M*. The Ricci operator *Q* is a tensor field of type (1,1) on *M* defined by

$$g(QX,Y) = S(X,Y) \tag{2}$$

for all vector fields on *TM.*

Let *M* be an *(2n+1)*- dimensional C^∞ manifold and $\chi(M)$ the Lie algebra of C^∞ vector fields on *M*. An almost contact structure on *M* is defined by (1,1) tensor field φ, a vector field ξ and a 1-form η on *M*. If (φ, ξ, η) satisfy the following condition then (φ, ξ, η) is said to be almost contact structure,

$$\eta(\xi) = 1, \quad \varphi^2 = -I + \eta \otimes \xi \tag{3}$$

$$\varphi\xi = 0, \quad \eta \circ \varphi = 0 \tag{4}$$

where *I* denotes the identity transformation of the tangent space T_pM at the point of *p*. Then *M* equipped with (φ, ξ, η) almost contact manifold. *M* with metric tensor *g* and with a triple (φ, ξ, η) such that

$$g(\varphi X, \varphi Y) = g(X,Y) - \eta(X)\eta(Y) \tag{5}$$

and

$$g(X,\xi) = \eta(X) \tag{6}$$

where $X, Y \in \chi(M)$, is an almost contact metric manifold.

Let $\left(M^{2n+1}, \varphi, \xi, \eta, g\right)$ be an almost contact metric manifold and $\Phi(X,Y) = g(X, \varphi Y)$ is the fundamental 2- form of *M. M* is called almost α -Kenmotsu manifold, if the 1- form η and the 2-form Φ satisfy the following conditions:

$$d\eta = 0, \quad d\Phi = 2\alpha\eta \wedge \Phi \tag{7}$$

α being a non-zero real constant (Janssens and Vanhecke, 1981).

We have known that an almost contact metric manifold $\left(M^{2n+1}, \varphi, \xi, \eta, g\right)$ is said to be normal if the Nijenhius tensor

$$N_\varphi(X,Y) = [\varphi X, \varphi Y] - \varphi[\varphi X, Y] - \varphi[X, \varphi Y] + \varphi^2[X,Y] + 2d\eta(X,Y)\xi$$

vanishes for any $X, Y \in \chi(M)$. Remarking that a normal almost α -Kenmotsu manifold is said to be α -Kenmotsu manifold $(\alpha \neq 0)$ (Janssens and Vanhecke, 1981). Moreover, if the manifold *M* satisfies the following relations

$$(\nabla_X \varphi)Y = \alpha\{- g(X, \varphi Y)\xi - \eta(Y)\varphi X\} \tag{8}$$

and

$$\nabla_X \xi = \alpha(X - \eta(X)\xi) \tag{9}$$

then $\left(M^{2n+1}, \varphi, \xi, \eta, g\right)$ is called α -Kenmotsu manifold (Pitiş, 2007).

A Riemannian manifold *(M,g)* is called a $\varphi - $ recurrent Riemannian manifold, if the curvature tensor *R* satisfies the following condition:

$$\varphi^2\left((\nabla_W R)(X,Y)Z\right) = A(W)R(X,Y)Z \tag{10}$$

where *A* is 1-form (De et al., 2009; Yıldız et al., 2009).

A Riemannian manifold *(M,g)* is called $\varphi - $ Ricci symmetric, if its Ricci tensor *S* satisfies the following condition:

$$\varphi^2[(\nabla_X Q)Y] = 0 \tag{11}$$

for all vector fields *X* and *Y* in *TM* (Shukla and Shukla, 2009). A Riemannian manifold M is said to be locally $\varphi - $ symmetric, if

$$\varphi^2[(\nabla_W R)(X,Y)Z] = 0 \tag{12}$$

for all vector fields *X,Y,Z,W* orthogonal to ξ. This notion was introduced by Takahashi (Binh et al., 2002), for a Sasakian manifold.

A Riemannian manifold *(M,g)* is called quasi-conformally flat if its quasi-conformal curvature tensor $\overline{C}$,

$$\overline{C}(X,Y)Z = aR(X,Y)Z + b\left\{\begin{matrix} S(Y,Z)X - S(X,Z)Y + g(Y,Z)QX \\ - g(X,Z)QY \end{matrix}\right\}$$
$$- \frac{r}{2n+1}\left(\frac{a}{2n} + 2b\right)[g(Y,Z)X - g(X,Z)Y] \tag{13}$$

satisfies $\overline{C} = 0$, where r is the scalar curvature of *(M,g)*.
A Riemannian manifold *(M,g)* is called concircularly flat if its concircular curvature tensor Z,

$$Z(X,Y)W = R(X,Y)W - \frac{r}{2n(2n+1)}\{g(Y,W)X - g(X,W)Y\}$$

satisfies *Z=0*, where *r* is the scalar curvature of *(M,g)*.
On an $\alpha - $ Kenmotsu manifold *M,* the following relations are held (Janssens and Vanhecke, 1981):

$$S(X,\xi) = -2n\alpha^2\eta(X) \tag{14}$$

$$R(\xi,X)Y = \alpha^2\left[-g(X,Y)\xi + \eta(Y)X\right] \tag{15}$$

$$R(X,Y)\xi = \alpha^2\left[\eta(X)Y - \eta(Y)X\right] \tag{16}$$

$$S(\varphi X, \varphi Y) = S(X,Y) + \alpha^2 2n\eta(X)\eta(Y) \tag{17}$$

$$(\nabla_X\eta)Y = \alpha\left[g(X,Y) - \eta(X)\eta(Y)\right] \tag{18}$$

φ -RECURRENT $\alpha -$ KENMOTSU MANIFOLDS

Here, we find that a $\varphi - $ recurrent $\alpha - $ Kenmotsu manifold is an $\eta - $ Einstein manifold.

Theorem

A $\varphi - $ recurrent $\alpha - $ Kenmotsu manifold is an $\eta - $ Einstein manifold (Dogan, 2014).

Proof

Let (M,φ,ξ,η,g) be a $\varphi - $ recurrent $\alpha - $ Kenmotsu manifold. In this case; Riemannian curvature tensor of *M* satisfy the following equation for all *X,Y,Z* and *W* in *TM:*

$$\varphi^2\left[(\nabla_W R)(X,Y)Z\right] = A(W)R(X,Y)Z$$

From Equation (3), we get

$$(\nabla_W R)(X,Y)Z + \eta\left[(\nabla_W R)(X,Y)Z\right]\xi = A(W)R(X,Y)Z \tag{19}$$

for all X,Y,Z,W in *TM.* If we take the inner product of Equation (19) with $U \in \chi(M)$, we find

$$A(W)g(R(X,Y)Z,U) = -g((\nabla_W R)(X,Y)Z,U) + \eta((\nabla_W R)(X,Y)Z)\eta(U) \tag{20}$$

for all *X,Y,Z,W,U* in *TM.* Then the sum for $1 \le i \le 2n+1$ of the relation (20) with $X = U = e_i$ fields

$$A(W)S(Y,Z) = -(\nabla_W S)(Y,Z) + \eta\left[(\nabla_W R)(\xi,Y)Z\right]. \tag{21}$$

If we write ξ instead of *Z*, we get

$$A(W)S(Y,\xi) = -(\nabla_W S)(Y,\xi) + \eta\left[(\nabla_W R)(\xi,Y)\xi\right]. \tag{22}$$

From Equations (9), (14) and (16), we get

$$-2n\alpha^2 A(W)\eta(Y) = (2n+1)\alpha^3 g(W,Y) + \alpha S(Y,W) - \alpha^3\eta(W)\eta(Y). \tag{23}$$

If we write φY and φW instead *Y* and *W,* respectively, we find

$$0 = (2n+1)\alpha^3 g(\varphi W,\varphi Y) + \alpha S(\varphi Y,\varphi W), \tag{24}$$

From Equations (5) and (17), we have

$$S(Y,W) = -(2n+1)\alpha^2 g(Y,W) + \alpha^2\eta(Y)\eta(W) \tag{25}$$

for all *Y,W* in *TM.* Then , *M* is an $\eta - $ Einstein manifold.

$\varphi -$ RICCI SYMMETRIC $\alpha -$ KENMOTSU MANIFOLDS

Here, we find that a $\varphi - $ Ricci symmetric $\alpha - $ Kenmotsu manifold is an Einstein manifold.

Theorem

Let (M,φ,ξ,η,g) be a $\varphi - $ Ricci symmetric $\alpha - $ Kenmotsu manifold. Then *M* is an Einstein manifold.

Proof

Suppose that (M,φ,ξ,η,g) is a $\varphi - $ Ricci symmetric $\alpha - $ Kenmotsu manifold. In this case; Ricci operator of *M* satisfy the following condition:

$$\varphi^2\left[(\nabla_X Q)Y\right] = 0$$

for all *X,Y* in *TM.* Then, we find

$$-(\nabla_X Q)Y + \eta\left[(\nabla_X Q)Y\right]\xi = 0. \tag{26}$$

From this last equation, we have

$$-\nabla_X QY + Q\nabla_X Y + \eta(\nabla_X QY)\xi - \eta(Q\nabla_X Y)\xi = 0 \quad (27)$$

for all vector fields *X,Y* in *TM.* If we take the inner product of Equation (27) with $\xi \in \chi(M)$, then we find

$$-g(\nabla_X QY, \xi) + g(Q\nabla_X Y, \xi) + \eta(\nabla_X QY) - \eta(Q\nabla_X Y)\xi = 0 \,(28)$$

and we continue the process, we get

$$S(\nabla_X Y, \xi) - \eta(Q\nabla_X Y) = 0$$
$$-2n\alpha^2\eta(\nabla_X Y) = \eta(Q\nabla_X Y)$$
$$g(-2n\alpha^2\nabla_X Y, \xi) = g(Q\nabla_X Y, \xi) \quad (29)$$

for all *X,Y* in *TM.* From Equations (2) and (29)

$$Q = -2n\alpha^2$$

and

$$QX = -2n\alpha^2 X$$

for all *X* in *TM.* In this case, we have

$$S(X,Y) = g(QX,Y)$$
$$= g(-2n\alpha^2 X, Y)$$
$$= -2n\alpha^2 g(X,Y)$$

for all *X,Y* in *TM.* Then the proof is complete.

LOCALLY $\varphi-$ SYMMETRIC $\alpha-$ KENMOTSU MANIFOLD

Here, we prove that locally $\varphi-$ symmetric $\alpha-$ Kenmotsu manifolds have constant scalar curvature. In addition to if this type manifolds are quasi-conformal flat, then the manifold is Einstein manifold. On the other hand, we find that if locally $\varphi-$ symmetric $\alpha-$ Kenmotsu manifolds are concircular flat, then these manifolds have constant curvature and their curvature is given $\frac{r}{2n(2n+1)}$ (*r* is scalar curvature of *M).*

Lemma 1

Let $(M, \varphi, \xi, \eta, g)$ be a locally $\varphi-$ symmetric $\alpha-$ Kenmotsu manifold. Then scalar curvature of *M* is constant .

Proof

Suppose that $(M, \varphi, \xi, \eta, g)$ is a locally $\varphi-$ symmetric $\alpha-$ Kenmotsu manifold. That is; Riemannian curvature tensor of *M* satisfy the following equation

$$\varphi^2[(\nabla_W R)(X,Y)Z] = 0$$

where *X,Y,Z* and *W* are orthogonal to ξ. If we continue the process, we obtain

$$-(\nabla_W R)(X,Y)Z + \eta[(\nabla_W R)(X,Y)Z]\xi = 0 \qquad (30)$$

for all *X,W,Z* orthogonal to ξ. Then the sum for $1 \le i \le 2n+1$ of the relation (30), we get

$$(\nabla_W S)(X,Z) + \eta((\nabla_W R)(X,\xi)Z) = 0 \,.$$

In this case;

$$(\nabla_W S)(X,Z) + \eta\begin{bmatrix} \nabla_W R(X,\xi)Z - R(\nabla_W X, \xi)Z \\ - R(X, \nabla_W \xi)Z - R(X,\xi)\nabla_W Z \end{bmatrix} = 0$$

for all *X,W,Z* orthogonal to ξ. So, using Equations (9) and (15), we obtain,

$$(\nabla_W S)(X,Z) + \alpha^2 g(X,Z)\eta(\nabla_W \xi) - \alpha^2\eta(Z)\eta(\nabla_W X)$$
$$+ \alpha^2 g(\nabla_W X, Z) - \alpha^2\eta(Z)\eta(\nabla_W X) - \alpha\eta(R(X,W)Z)$$
$$+ \alpha\eta(R(X,W)Z) - \alpha\eta(W)\eta(R(X,\xi)Z) - \alpha\eta(W)\eta(R(X,\xi)Z)$$
$$- \eta(R(X,\xi)\nabla_W Z) = 0.$$

If we continue the process, we get

$$(\nabla_W S)(X,Z) = -\alpha^2 g(\nabla_W X, Z) + \alpha^2 g(\nabla_W Z, X) + \alpha^3\eta(W)g(X,Z)$$
$$-\alpha^3\eta(W)\eta(X)\eta(Z) - \alpha^2\eta(X)\eta(\nabla_W Z). \qquad (31)$$

M is locally $\varphi-$ symmetric, so

$$\eta(X) = \eta(Y) = \eta(W) = \eta(Z) = 0 \,.$$

Then we find

$$(\nabla_W S)(X,Z) = -\alpha^2 g(\nabla_W X, Z) + \alpha^2 g(\nabla_W Z, X). \quad (32)$$

If we write $X = Z = e_i$ and we take the sum for $1 \le i \le 2n+1$ of the relation (32), we obtain

$$dr(W) = 0$$

for all vector fields *W* in *TM.* Then, the proof is complete.

Theorem

Let $(M, \varphi, \xi, \eta, g)$ be a locally φ-symmetric α-Kenmotsu manifold. If *M* is quasi-conformally flat, then *M* is Einstein manifold.

Proof

Suppose that $(M, \varphi, \xi, \eta, g)$ is a locally φ-symmetric α-Kenmotsu manifold. Then $\overline{C}(X,Y)Z$ quasi-conformal curvature tensor of *M* vanishes for any *X,Y,Z* in *TM.* That is,

$$aR(X,Y)Z + b[S(Y,Z)X - S(X,Z)Y + g(Y,Z)QX - g(X,Z)QY]$$
$$- \frac{r}{2n(2n+1)}\left(\frac{a}{2n} + 2b\right)[g(Y,Z)X - g(X,Z)Y] = 0$$
(33)

for all *X,Y,Z* in *TM.* If we write ξ instead of *X* and *Z* and later we take the inner product of Equation (33) with $W \in \chi(M)$, then we get

$$S(Y,W) = \frac{1}{b}\left\{a\alpha^2 + 2nb\alpha^2 + \frac{r}{2n+1}\left(\frac{a}{2n} + 2b\right)\right\}g(Y,W)$$
$$+ \frac{1}{b}\left\{-a\alpha^2 - 4nb\alpha^2 - \frac{r}{2n+1}\left(\frac{a}{2n} + 2b\right)\right\}\eta(Y)\eta(W).$$
(34)

If we use Lemma 1 and we consider locally φ-symmetric then *r* is constant and $\eta(Y) = \eta(W) = 0$ since *Y* and *W* orthogonal to ξ. So we have

$$S(Y,W) = \lambda g(Y,W)$$

$(\lambda = \frac{1}{b}\left\{a\alpha^2 + 2nb\alpha^2 + \frac{r}{2n+1}\left(\frac{a}{2n} + 2b\right)\right\})$. In this case, *M* is Einstein Manifold.

Theorem

Let *M* be a locally φ-symmetric α-Kenmotsu manifold. If *M* is concircularly flat then *M* has got constant curvature and its curvature is $\frac{r}{2n(2n+1)}$.

Proof

Suppose that *M* is a locally φ-symmetric α-Kenmotsu

manifold. If *M* is concircularly flat then we obtain

$$R(X,Y)W = \frac{r}{2n(2n+1)}\{g(Y,W)X - g(X,W)Y\}. \quad (35)$$

If we consider Lemma 1 and the Equation (35), then we complete the proof.

Example

$M = \{(x,y,z) \in R^3, (x,y,z) \neq (0,0,0)\}$, where (x,y,z) are the standard coordinates in R^3. The vector fields

$$e_1 = \alpha z \frac{\partial}{\partial x} \qquad e_2 = \alpha z \frac{\partial}{\partial y} \qquad e_3 = -\alpha z \frac{\partial}{\partial z}$$

are linearly independent at each point of *M.* Let *g* be Riemannian metric defined by

$$g = \frac{dx^2 + dy^2 + dz^2}{\alpha^2 z^2}.$$

Then we find

$$g(e_1, e_3) = g(e_1, e_2) = g(e_2, e_3) = 0$$
$$g(e_1, e_1) = g(e_2, e_2) = g(e_3, e_3) = 1.$$

Let η be the 1-form defined by $\eta(X) = g(X, e_3)$ for any $X \in \chi(M)$. Let φ be a $(1,1)$ tensor field defined by $\varphi(e_1) = -e_2$, $\varphi(e_2) = e_1$, $\varphi(e_3) = 0$. If we define $\xi = e_3$, $\eta(X) = g(X, e_3)$ for all vector fields *X* in *TM* and use the linearity of φ and *g*, then we find

$$\eta(\xi) = 1, \quad \varphi^2 X = -X + \eta(X)\xi, \quad g(\varphi X, \varphi Y) = g(X,Y) - \eta(X)\eta(Y)$$

for all vector fields *X, Y* in *TM.* In this case, $(M, \varphi, \xi, \eta, g)$ is an almost contact metric manifold. Suppose that ∇ is Levi-Civita connection with respect to the metric *g.* For all $f \in C(R^3, R)$, we get

$$[e_1, e_2]f = e_1(e_2(f)) - e_2(e_1(f))$$
$$= e_1(\alpha z f_y) - e_2(\alpha z f_x)$$
$$= 0$$

$$[e_1,e_3]f = e_1(e_3(f)) - e_3(e_1(f))$$
$$= e_1(-\alpha z f_z) - e_3(\alpha z f_x)$$
$$= \alpha z(-\alpha z f_{zx}) + \alpha z(\alpha z f_{xz} + \alpha f_x)$$
$$= \alpha e_1(f)$$

and

$[e_2,e_3]f = \alpha e_2(f)$. In this case, from Kozsul's Formula, we find

$$\nabla_{e_1}e_1 = -\alpha e_3 \quad \nabla_{e_2}e_1 = 0 \quad \nabla_{e_3}e_1 = 0$$
$$\nabla_{e_1}e_2 = 0 \quad \nabla_{e_2}e_2 = -\alpha e_3 \quad \nabla_{e_3}e_2 = 0$$
$$\nabla_{e_1}e_3 = \alpha e_1 \quad \nabla_{e_2}e_3 = \alpha e_2 \quad \nabla_{e_3}e_3 = 0.$$

Let $X = ae_1 + be_2 + c\xi$ and $Y = \bar{a}e_1 + \bar{b}e_2 + \bar{c}\xi$ be vector fields in *TM* (Where $a,b,c,\bar{a},\bar{b},\bar{c} \in R$). Then we get $\varphi Y = \bar{b}e_1 - \bar{a}e_2$. In this case;

$$(\nabla_X \varphi)Y = \nabla_X \varphi Y - \varphi \nabla_X Y$$
$$= \nabla_{ae_1+be_2+c\xi}(\bar{b}e_1 - \bar{a}e_2) - \varphi(\nabla_{ae_1+be_2+c\xi}(\bar{a}e_1 + \bar{b}e_2 + \bar{c}\xi))$$
$$= \alpha\{-(a\bar{b} - b\bar{a})\xi - \bar{c}(-ae_2 + be_1)\}$$
$$= \alpha\{-g(X,\varphi Y)\xi - \eta(Y)\varphi X\}$$

for all vector fields *X,Y* in *TM*. Hence (M,φ,ξ,η,g) is an α − Kenmotsu manifold. With the help of above results we can find the following:

$$g(R(e_1,X)Y,e_1) = -\alpha^2(b\bar{b} + c\bar{c})$$
$$g(R(e_2,X)Y,e_2) = -\alpha^2(a\bar{a} + c\bar{c})$$
$$g(R(e_3,X)Y,e_3) = -\alpha^2(a\bar{a} + b\bar{b})$$

and

$$S(X,Y) = \sum_{i=1}^{2n+1} R(e_i,X,Y,e_i)$$
$$S(X,Y) = -\alpha^2 g(X,Y) - \alpha^2 \eta(X)\eta(Y).$$

Hence, *M* is an η − Einstein manifold. Now, we take *X,Y,Z* and *W* orthogonal to ξ. Then we can write

$$X = ae_1 + be_2$$
$$Y = \bar{a}e_1 + \bar{b}e_2$$
$$Z = \tilde{a}e_1 + \tilde{b}e_2$$
$$W = \hat{a}e_1 + \hat{b}e_2.$$

In this case, if we compute $(\nabla_W R)(X,Y)Z$, we find

$$(\nabla_W R)(X,Y)Z = \nabla_W R(X,Y)Z - R(\nabla_W X,Y)Z - R(X,\nabla_W Y)Z - R(X,Y)\nabla_W Z$$
$$= 0.$$

Then,

$$\varphi^2(\nabla_W R)(X,Y)Z = 0$$

for all vector fields *X,Y,Z* and *W* orthogonal to ξ. In this case, this manifold is a locally φ − symmetric α − Kenmotsu manifold. In Lemma 1, we show that scalar curvature of a locally φ − symmetric α − Kenmotsu manifold is constant. Actually, if we compute scalar curvature for all vector fields *X,Y* orthogonal to ξ, we see that

$$S(X,Y) = -\alpha^2 g(X,Y)$$
$$r = \sum_{i=1}^{3} S(e_i,e_i) = -3\alpha^2 .$$

Conflict of Interest

The authors have not declared any conflict of interest.

ACKNOWLEDGEMENT

REFERENCES

Besse AL (1987). Einstein Manifolds. Classics in Mathematics. Berlin: Springer. ISBN 3-540-74120-8. http://dx.doi.org/10.1007/978-3-540-74311-8

Binh TQ, Tamassy L, De UC, Tarafdar M (2002). Some remarks on almost Kenmotsu manifolds. Mathematica Pannonica, 13:31-39.

De K (2014). On a Class of β − Kenmotsu manifolds. Facta Univarsitatis 29(2):173-188.

De UC, Yıldız A, Yalınız AF (2009). On φ -recurrent Kenmotsu manifolds. Turkey J. Math. 33:17-25.

Dileo G (2011). A classification of certain almost α − Kenmotsu Manifolds. Kodai Math. J. 34(3): 426-445. http://dx.doi.org/10.2996/kmj/1320935551

Dogan S (2014). On some special kenmotsu structures. Ph.D. Thesis, Inonu University, Malatya/Turkey.

Janssens D, Vanhecke L (1981). Almost contact structures and curvature tensors. Kodal Math. J. 4: 1-27. http://dx.doi.org/10.2996/kmj/1138036310

Oubina JA (1985). New class of almost contact metric manifolds. Publ. Math. Debrecen 32:187-193.

Öztürk M, Aktan N, Murathan C (2010). On α-Kenmotsu manifolds satisfying certain conditions. Balkan Soc. Geometers, 12:115-126.

Pitiş G (2007). Geometry of Kenmotsu manifolds, Publishing House of Transilvania University of Braşov, Braşov.

Shukla SS, Shukla MK (2009). On φ-Ricci symmetric Kenmotsu manifolds. Novi Sad J. Math. 39(2):89-95.

Yano K (1940). Concircular geometry I. Concircular transformations, Proc. Imp. Acad. Tokyo 16:195-200. http://dx.doi.org/10.3792/pia/1195579139

Yıldız A, De UC, Acet BE (2009). On Kenmotsu manifolds satisfying certain curvature condition. SUT J. Math. 45(2):89-101.

Full Length Research Paper

Analysis and evaluation of differential inductive transducers for transforming physical parameters into usable output frequency signal

A. Deji, S. Khan*, M. M. Ahmed, J. Chebil and A. H. M. Z. Alam

Department of Electrical and Computer Engineering, International Islamic University, Malaysia.

This paper presents a novel hybrid oscillating inductive sensor circuit converting deflection oscillations into useful signal and thus being used to support an oscillatory circuit mechanism and management of their resulting oscillation in a real-time implementation. This circuit does not only detects and optimizes the deflections produced in an oscillation in instrumentation electronics, but also provide an improved sensory with high accuracy, sensitivity, responsiveness and operating range. The design therefore help in transforming the deflection deviations in the in and out movement of the core into useful output content. A simulation and derivation of the oscillating circuit in see-saw convulsion bar sensing system has been implemented. Simulation and derivations shows how the oscillating circuits of the bar are converted into frequency, duty cycle, current, voltages for further wireless applications.

Key words: Differential inductive sensing, displacement inductance-to-frequency converter, deflection deviation, see-saw bar, oscillation, position sensing.

INTRODUCTION

Sensors have proven important in converting immeasurable quantities such as wind velocity, vibrations, oscillation, turning effects of forces, deviations, illness etc into qualitative and quantitative electrical signal suitable for real time implementation by an intelligent oscillation harvesting mechanism. For an accurate measurement of such oscillation parameter, an efficient oscillation detector is essential (Figure 1).

This is capable of converting a see-saw convulsion bar into frequency response, duty cycle response, voltage response. The sensor output should be such that the oscillation/vibration, their motion, damping etc is determined. Based on the sensing inductive principle

used, the designed circuit can be categorized into a vibration sensor and pressure sensor applied even in height location such as; sagging and oscillations of electrical transmission line, turning moment in railroad, signal upgrade from degradation in GSM mask (Ezzat and Cheng, 2011; Edgarcio et al., 1988; Grover and Deller, 1999; Hameed et al., 2012).

The sensor output should be such that electro-mechanical deviations in oscillation circuit and their effects servomechanism are determined. The vibration *sensor can be categorized according to the sensing* element such as resistive, capacitive, inductive and linear variable differential transducer (Mohammed et al., 2012;
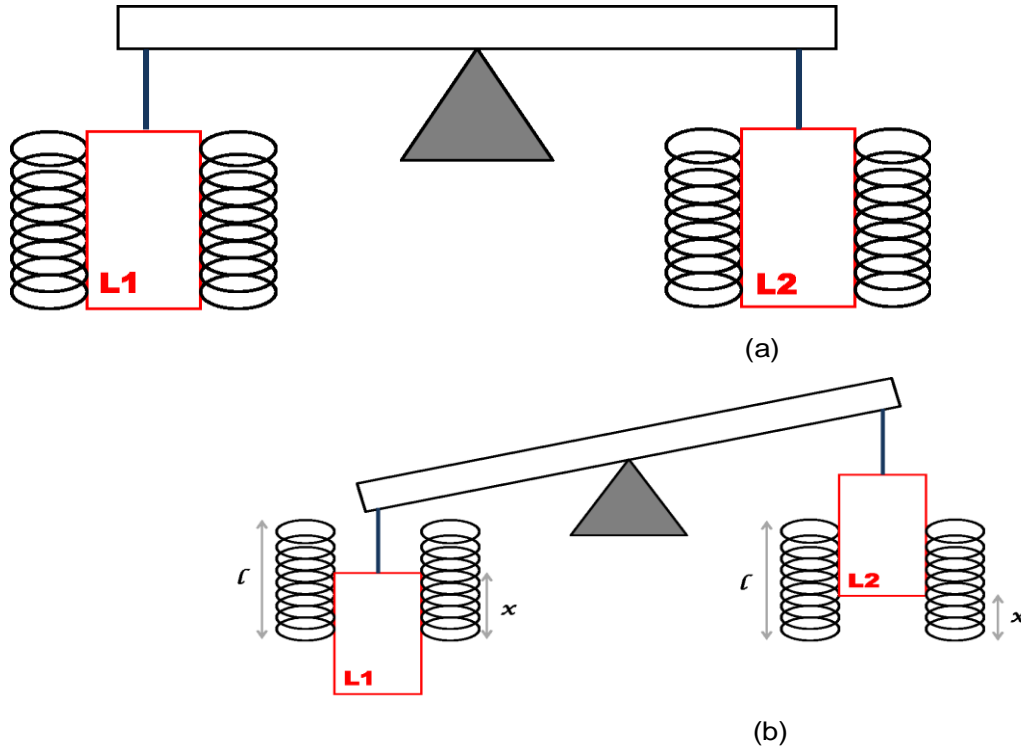
Figure 1. (a) A balance see-saw of overhanging bar, (b) Differential manner of an overhanging see-saw bar.

Mohan et al., 2008). Piezo-resistive sensors have good linearity and acceptable sensitivity, but suffer from the problem of inaccuracies (Mohan et al., 2009; Ravindra, 2006). Capacitive pressure/oscillation sensors exhibit features of higher sensitivity and lower temperature hysteresis, but they are usually nonlinear (Ravindra, 2006; Saxena and Sahu, 1994; Slamwomir, 2007). Conventional LVDT-based pressure/oscillation sensors possess good linearity, highest sensitivity and lowest temperature hysteresis, but such devices have got bulky physical structures (Saxena and Sahu, 1994; Slamwomir, 2007; Texas Instruments, "LM555 Data sheet", 2003; Udaya and Duleepa, 2011). This paper presents a sensor capable of harnessing oscillations in circuits into pulse able signal. Each aspect of this finding has been put into different sections.

STRUCTURAL MODEL AND DESIGN

The structure of the proposed oscillating circuit is shown schematically in Figure 2. The oscillation of the actual component of the sensor varying differentially, maximizing the circuit variations and deviations into a derivable and pulse able signal is shown in Figure 3. As shown in Figures 2, 3 and 4, a vertical core of a varying height of 4 to 36 mm is embedded into an open stator made up of magnetic coils thereby providing the inductive change in relation to circuit vibrations. The oscillation of the circuit provides the force or pressure needed to bring about the inductance of the

coil as the core is displaced in and out of the coils mounted in a stator of a servomechanism. This displacement is proportional to the force or pressure and the inductance of the core. The timer circuit when connected to the coils in Figures 1 and 2 will give rise to Figures 3 and 4. This RL3R circuit gives us a square wave with a frequency depending on the inductance value of the coil as shown in Figure 5.

MATHEMATICAL MODEL OF THE CIRCUIT

A differential transducer is one that simultaneously senses two separate sources and provides an output proportional to the difference between the sensing. Considering the idea in Figure 4, the inductances of the two coils change in a differential manner when the overhanging bar is moving in a seesaw manner. At position 'x', the inductance of the right hand side of the coil is given by Equation (1), while that of the left hand side is given by Equation (2), giving the total equation as follows:

$$L_{TOTAL} = \frac{\mu_0 N^2 A}{l}\left[\mu_r \frac{x}{l} + \frac{l-x}{l}\right] = \frac{\mu_0 N^2 A}{l}\left[1 + \frac{x}{l}(\mu_r - 1)\right] \tag{1}$$

$$L_{TOTAL} = \frac{\mu_0 N^2 A}{l}\left[\frac{x}{l} + \mu_r(\frac{l-x}{l})\right] = \frac{\mu_0 N^2 A}{l}\left[\mu_r + \frac{x}{l}(1 - \mu_r)\right] \tag{2}$$

Details of the derivation of equation 1 and 2 are shown in the APPENDIX A-1 to A-6. A linear relationship is shown in Figure 6 demonstrating the in and out oscillation of the device.
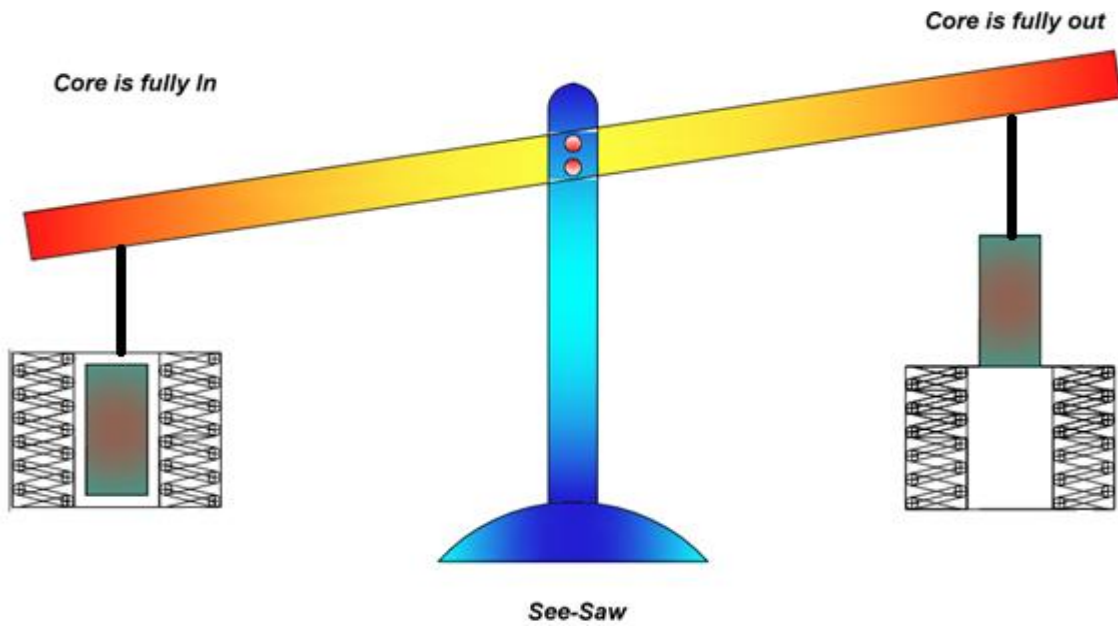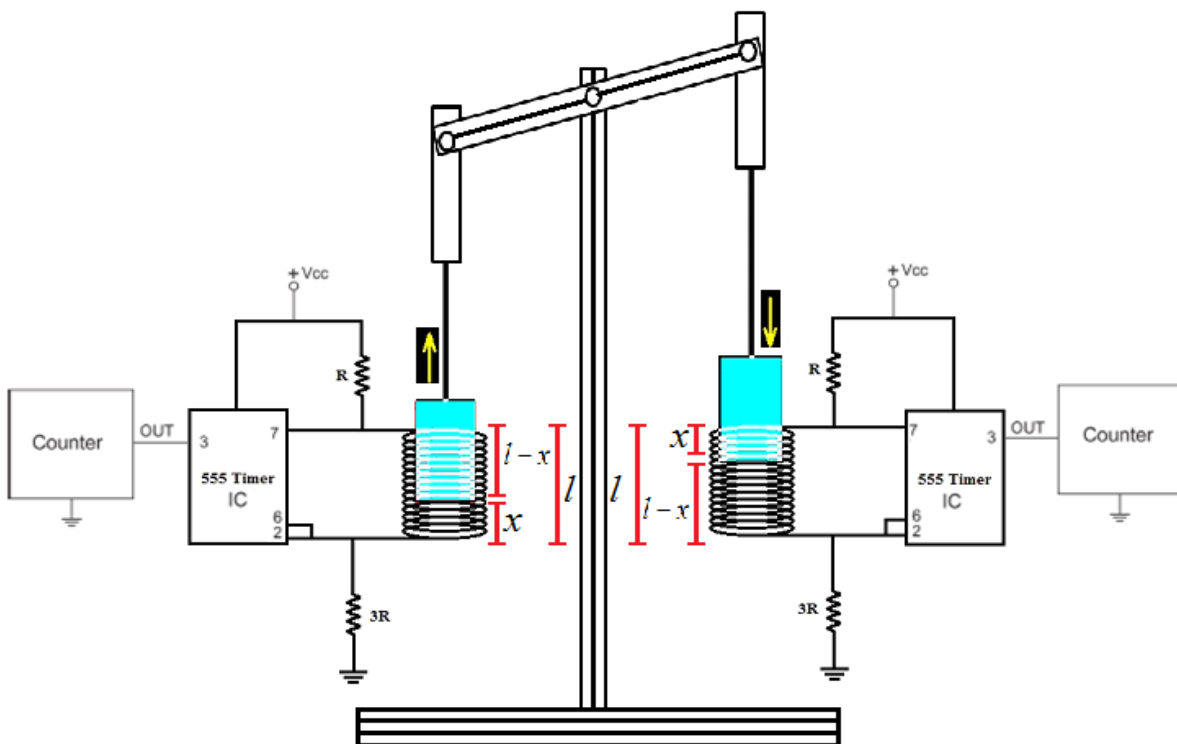
Figure 2. Varying differential cores in a see-saw.

Figure 3. Differential inductive system architecture.

Frequency output for inductive change delta L

The inductance of left inductor is given by L_1 and can be expressed as:

$L_1 = L_{fi} - \Delta L_1$

$\Delta L_1 = L_{fi} - L_1$

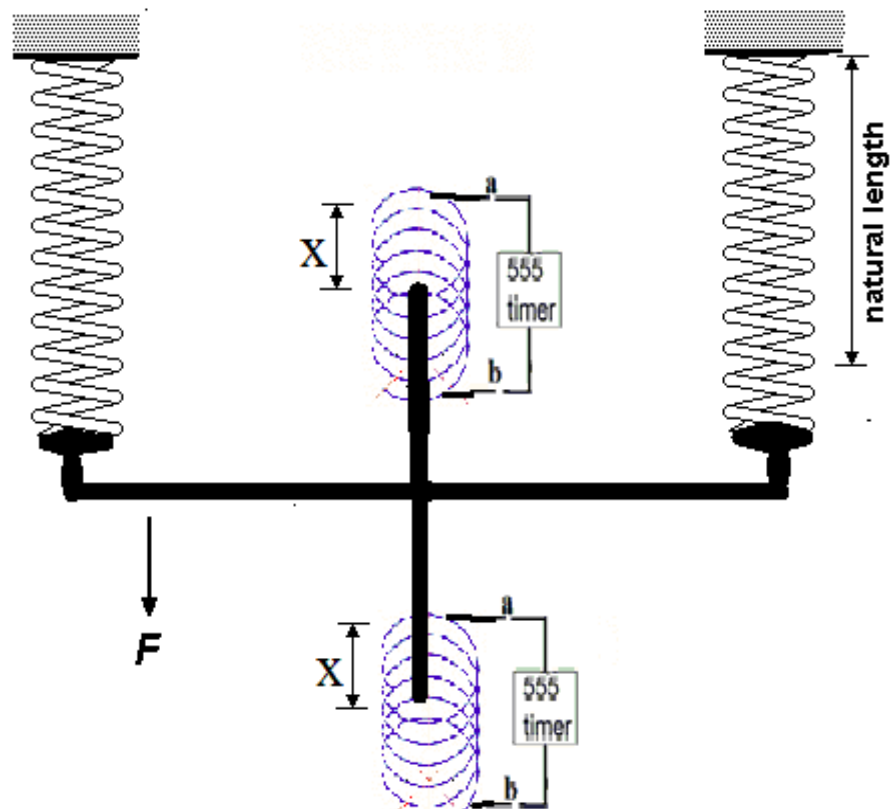Whereas the inductance of second inductor is given by L_2

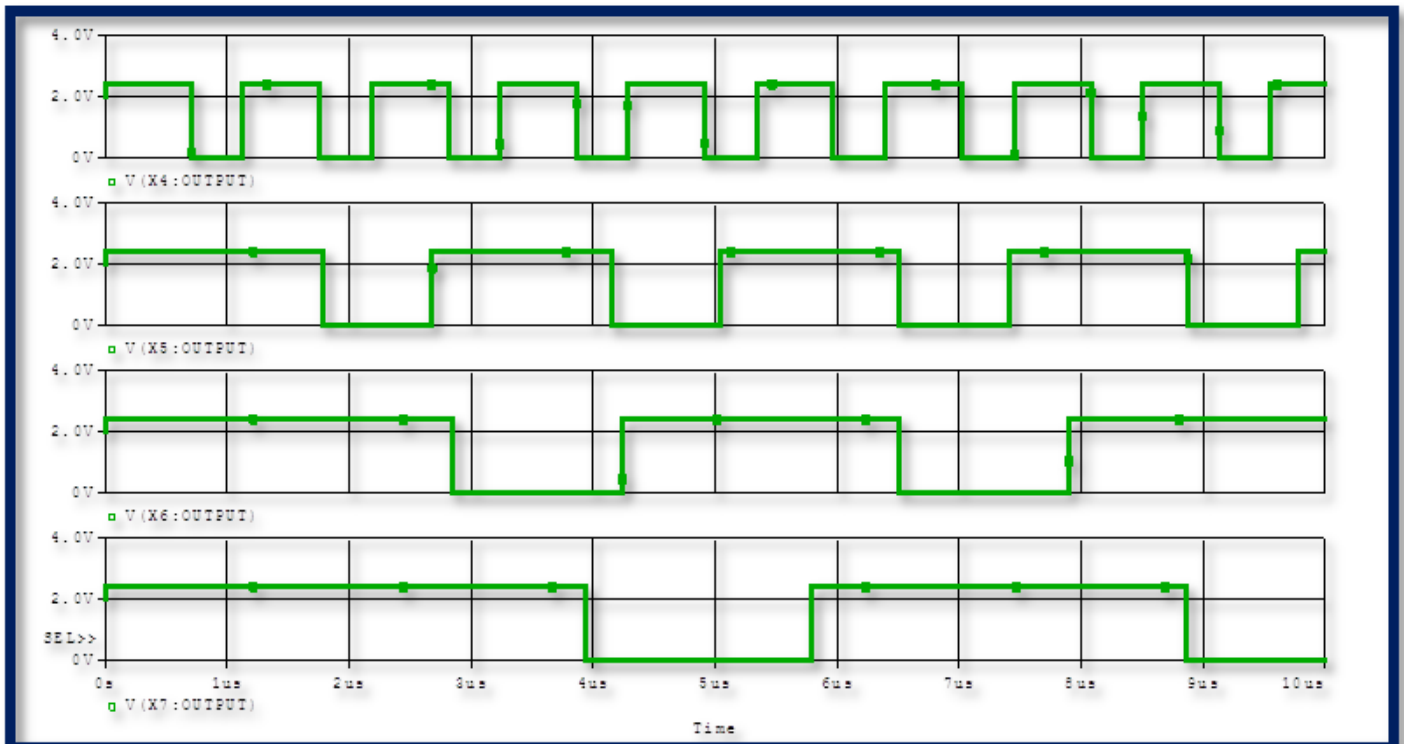**Figure 4.** Signal produced from circuit oscillation and vibrations.
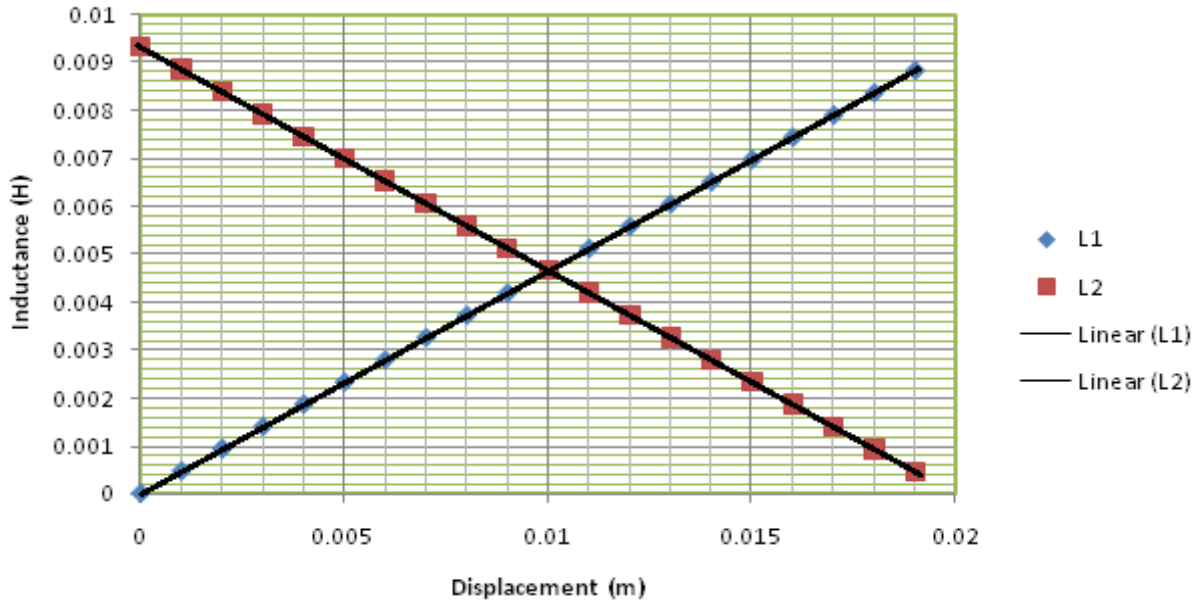

Figure 5. Voltage waveform from circuit oscillation.

Figure 6. A plot of the inductance variation with the displacement.

$L_2=L_{fo}+\Delta L_2$

$\Delta L_2=L_2-L_{fo}$

$\Delta L_{avg}=\frac{\Delta L1+\Delta L2}{2}$

The frequency of RL3R-timer circuit for single inductor is given by:

$f=1.58\frac{R}{L}$

The frequency of the first inductor is:

$f_1=1.58\frac{R}{Lfi-\Delta L1}$ (3)

The frequency of the second inductor is:

$f_2=1.58\frac{R}{Lfo+\Delta L2}$ (4)

The frequency of total inductive change is:

$\Delta f_1 = f_1 - f_{fi} = 1.58\,R\left(\frac{1}{L_1}-\frac{1}{L_{fi}}\right)$ (5)

$\Delta f_1 = 1.58\,R\left(\frac{L_{fi}-L_1}{L_1 L_{fi}}\right) = 1.58\,R\left(\frac{\Delta L1}{L_1 L_{fi}}\right)$

Substituting the value of L_1 in Equation (5) we get:

$\Delta f_1 = 1.58\,R\left(\frac{\Delta L1}{(Lfi-\Delta L1)\,L_{fi}}\right)$ (6)

Now solving for the other case of Δf_2, we obtain;

$\Delta f_2 = f_{fo} - f_2 = 1.58\,R(\frac{1}{L_{fo}}-\frac{1}{L_2})$ (7)

$\Delta f_2 = 1.58\,R\left(\frac{L_2-L_{fo}}{L_2 L_{fo}}\right) = 1.58\,R\left(\frac{\Delta L2}{L_2 L_{fo}}\right)$ (8)

Substituting the value of L_2 in Equation (7),

$\Delta f_2 = 1.58\,R\left(\frac{\Delta L1}{(Lfi-\Delta L1)\,L_{fi}}\right)$ (9)

$\Delta f_{avr} = \frac{\Delta L1+\Delta L2}{2}$ (10)

The plot for frequencies of the in and out movement of the core in the coil is given thus.

Frequency change as a function of displacement

From the previous equation, the frequency change as a function of displacement is given thus as:

$\Delta f_1 = 1.58\,R(\frac{l^2}{\mu_0\,N^2 A(1+x(\mu_r-1))}-\frac{1}{L_{fi}})$ (11)

That of the second coil is;

$\Delta f_2 = 1.58\,R(\frac{1}{L_{fo}}-\frac{l^2}{\mu_0\,N^2 A(\mu_r,1+x(1-\mu_r))})$ (12)

The plot for frequencies of the in and out movement of the core in the coil is given as; these change in frequencies from Equations (11) and (12), gives a symmetrical behaviour with respect to the displacement produced by the oscillatory motion of the core. This aforementioned behaviour gave rise the plot in Figure 7(a) showing the reciprocal behaviour of the in and out movement, harnessing the deviations in terms of oscillation in servomechanism and electro-mechanical devices. The frequency change with the displacement is given in Figure 7(b).
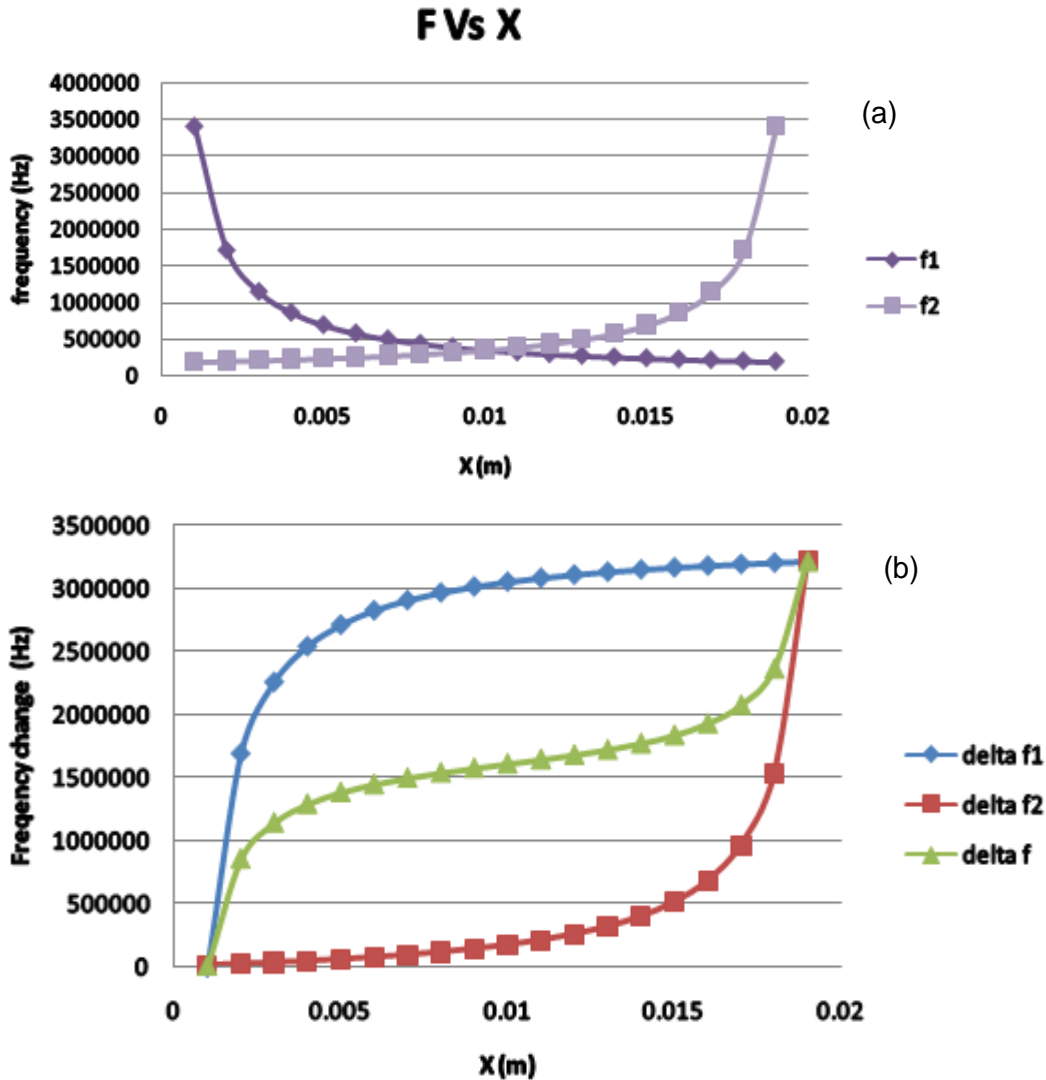
F Vs X

(a)

(b)

Figure 7. (a): A plot of Frequency change in symmetrical variation with respect to core displacement, (b): A plot of Frequency with respect to core displacement.

Frequency as a function of oscillations

Generally, vibrations in movement can be described or expressed by the following equations. In the case the seesaw bar shown in Figures 2 through 4, we assume that the seesaw bar in the springs has a movement which is a simple harmonic motion according to the following equation;

$$X = 0.5l - o.5l \cos (2\pi f_s t) \qquad (13)$$

The vibrations found in electronic circuit and in machines can be converted into useful frequencies as shown in Equations 14 and 15.

$$f_1 = \frac{1.58 \, R l^2}{\mu_0 \, N^2 A \left(l + [0.5l - o.5l \cos (2\pi f_s t)](\mu_r - 1)\right)} \qquad (14)$$

$$f_2 = \frac{1.58 \, R l^2}{\mu_0 \, N^2 A \left(\mu_r \, l + [0.5l - o.5l \cos (2\pi f_s t)](1 - \mu_r)\right)} \qquad (15)$$

To check the effect of the sea saw bar frequency, Equations (13), (14) and (15) are used. Assuming a coil of length of 20 mm, number of turns = 100, cross sectional area A=pi(r*r) where r=1 mm, an iron core with relative permeability 4728, and R= 1k ohm, then by changing the value of fs, the plots for the output frequency as a measure of x is obtained. Figure 8 shows the effect of the circuit as it oscillates, converting the deviations into these useful frequency values when the harmonics from the see-saw in the convulsion are given as 10, 100, 1000 and 10,000 Hz respectively.

SIMULATION RESULT AND ANALYSIS

A simulation of the designed mathematical model and its necessary derivations for frequency, frequency hysteresis, voltage and the current responses are carried out. The results obtained confirm the mathematical derivation plots with the simulation. Figure 9(a) is the
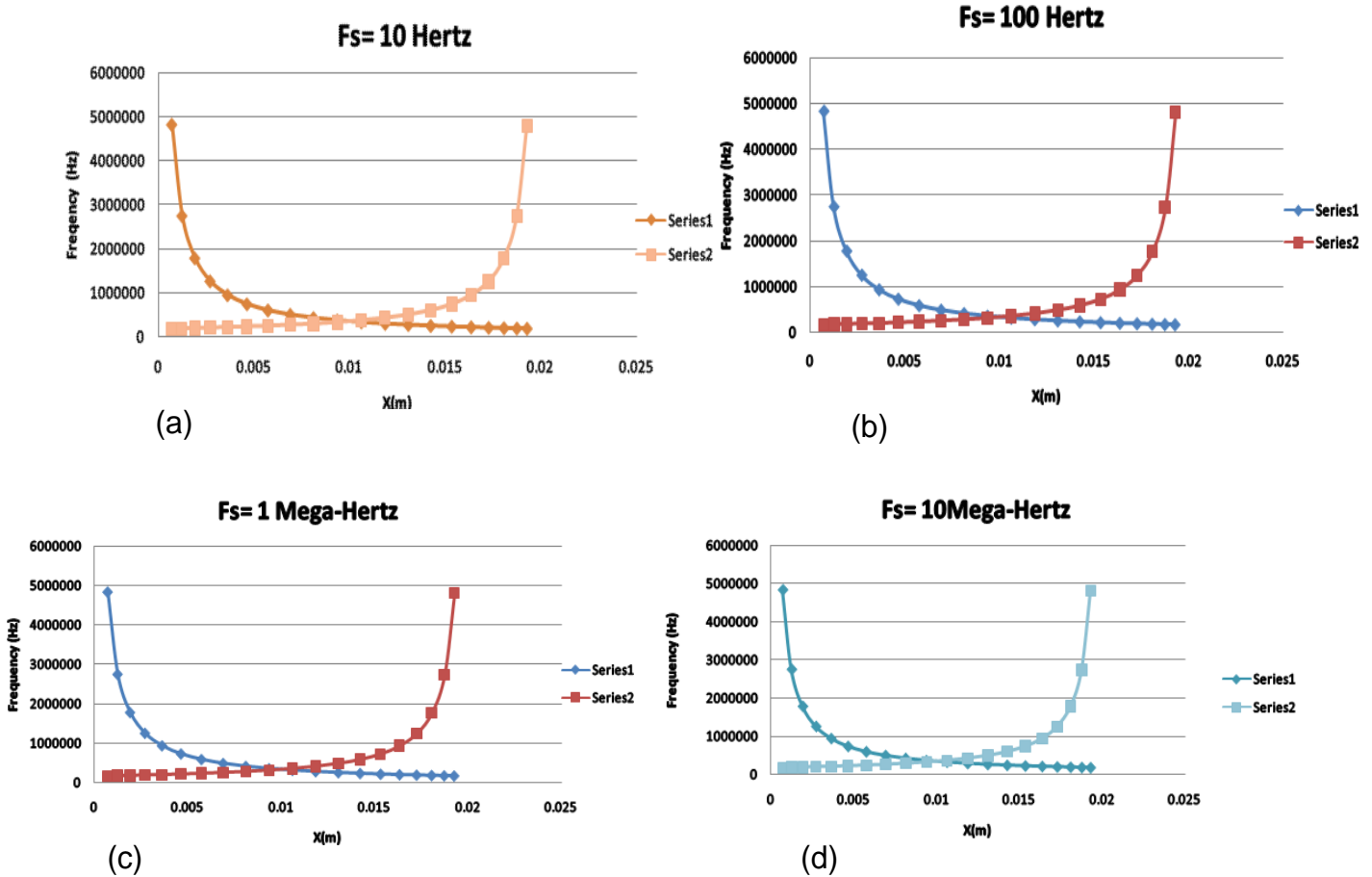
Figure 8. Plot of the Output Response for oscillating circuit for varying values of Fs.

result of simulation of both circuits; the right and the left one using the same assumption that was used in the calculations. The green line represents the frequency output of the left side and the red one is for the circuit in the right hand side as a measure of the core displacement. Figure 9(b) shows the output frequency when the sea saw frequency fs= 100 Hz, for three time periods, in every period, the displacement value change from 0 to l and from l to 0.

Figure 10(a) to (d) shows the result of simulation when the sea saw bar frequency is change. When the frequency of sea saw bar is 10 Hz, x changes from 0 to l, and time t, is changed from 0 to 50 ms, 0 to 100 ms, 0 to 1000 ms and 0 to 10000 ms according to Equation (15). The results obtained confirm those of the derivations shown in this work. A slight difference in simulation analytical deduction is due to the environmental effect on the circuit. The table for the different frequencies giving rise to frequency hysteresis is given in Table 1. This table gives rise to Figure 6, showing the frequencies of the see-saw behavior when the core is differentially in and out of its coil as the circuit oscillate.

A linear relationship exist between the inductance of the first coil, which increases when the core is moving in, while the core for the second coil is moving out, with decrease in inductance. The inductance change ΔL is calculated and plotted in Figure 6. These inductance change leads to a frequency change and hysteresis for the output of the timers as seen from derivations and simulation results. This shows that the frequency is decreasing when the core is going in and increases when the core goes out. At equilibrium state when the sea saw bar is horizontal, the displacement x is equal to half of the coil length, l and the value of the inductance for both coils is the same. This is clearly shown in Figure 6 at the point when x= 10 mm, the inductance L=4.67 mH for the two coils. The result of the inductance equality at this point is reflected to the frequency value as Figure 7.

The main difference between derivations and simulation result is seen when the coil is almost fully out. From derivation point, when the coil is fully out x=0, the frequency is larger than 800 Mega Hz, which is very large compared to other frequency values which ranges from 0.18 to 3.4 Mega Hz. On the other hand, simulation result
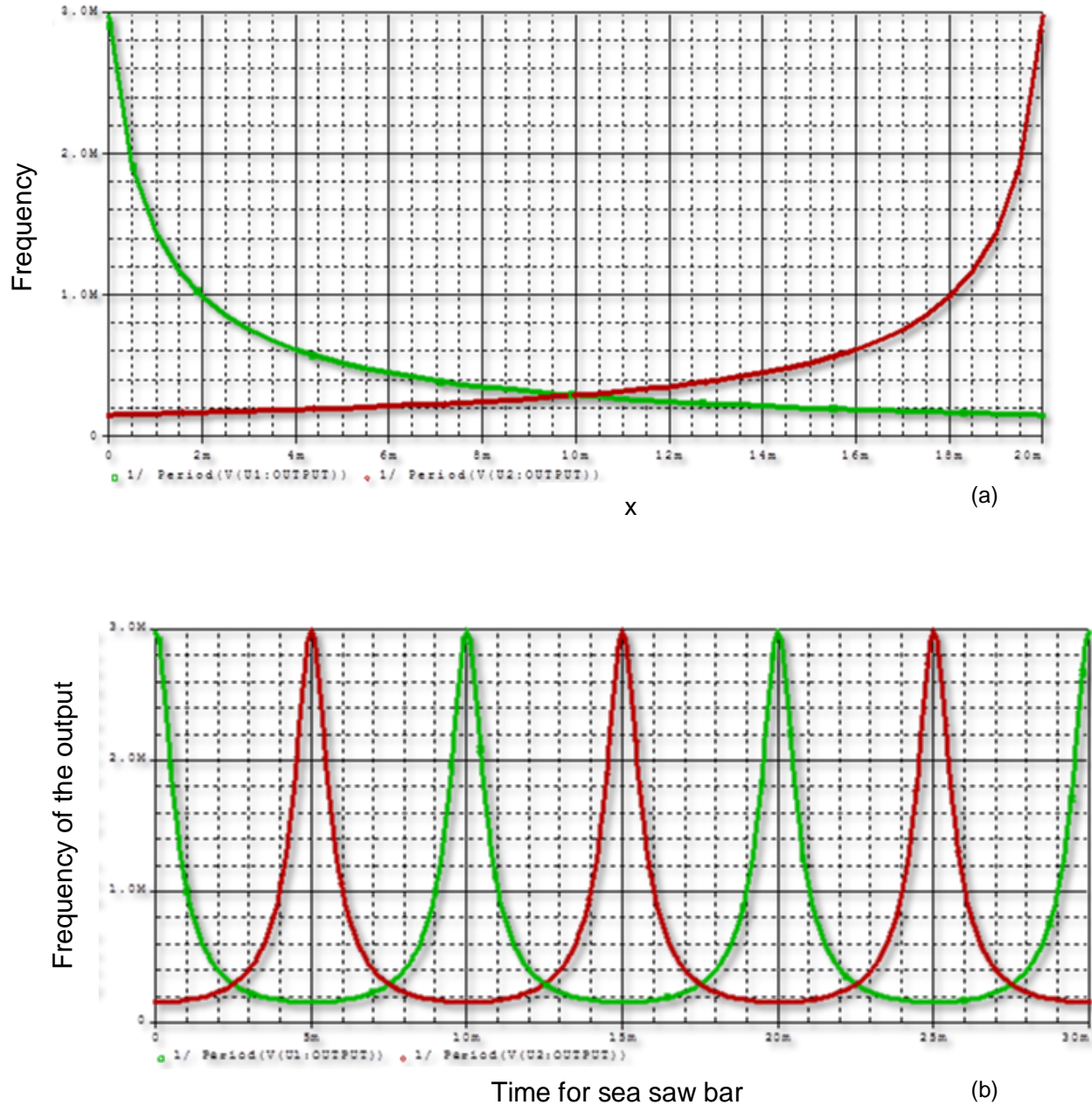
(a)

X

Time for sea saw bar

(b)

Figure 9. (a): A simulation of Frequency change in symmetrical variation with respect to core displacement, (b): Simulated Output for frequency with three time periods.

shows that maximum frequency occurs when the core is fully out and this is at 3 MHz as shown Figure 7. Although, the result from derivations and simulation has shown that the sea saw bar frequency has no effect on the output frequency values, the frequency counter calculate the value which is equal to the time period of the timer output for every reading. So, if the sea saw frequency fs exceeds a certain value, the frequency counter will give wrong frequency output. This value is derived as shown in Equation (16).
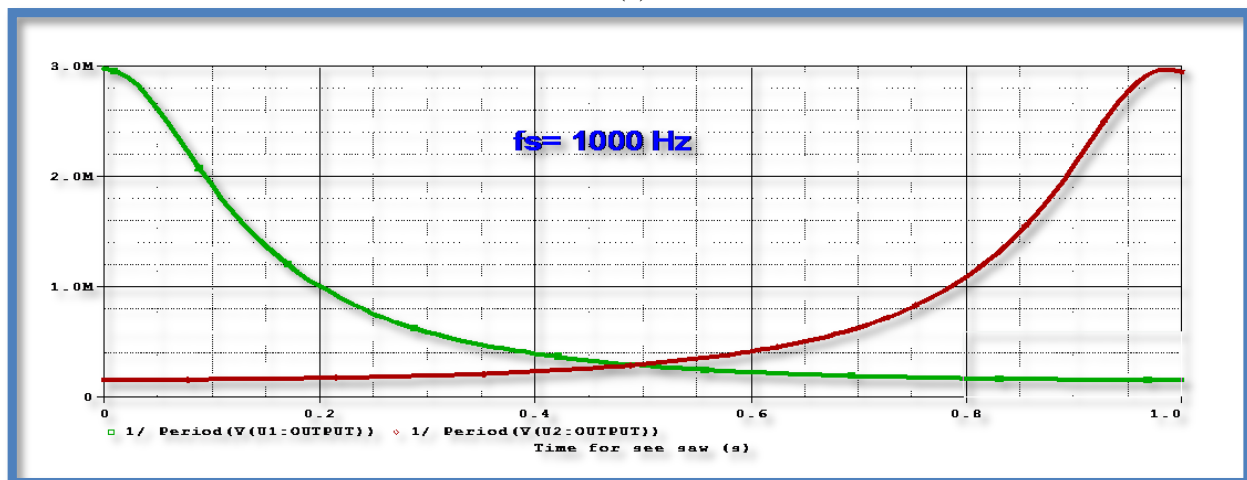
$$\sum_{x=0}^{x=l} 0.63 \, \frac{\mu_0 \, N^2 A}{R l^2} \, (\, l + x(\mu_r - 1)) \tag{16}$$
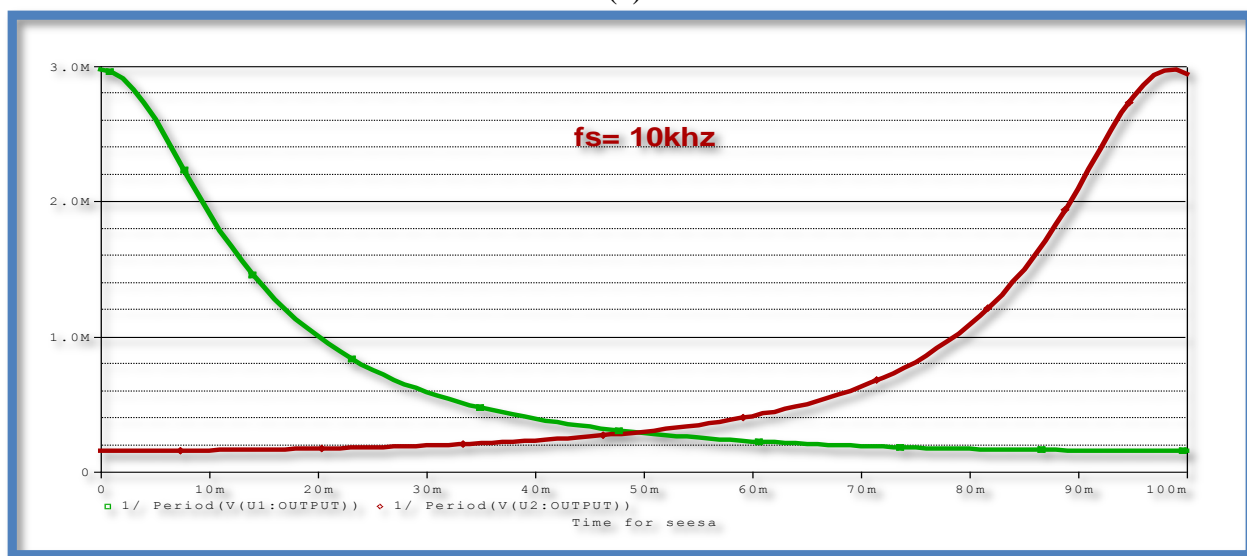
Conclusion

Differential sensing system architecture is proposed as shown in Figures 1 to 4. This consists of two coils with varying cores in which a change in the core position will result in inductance change. These changes can be
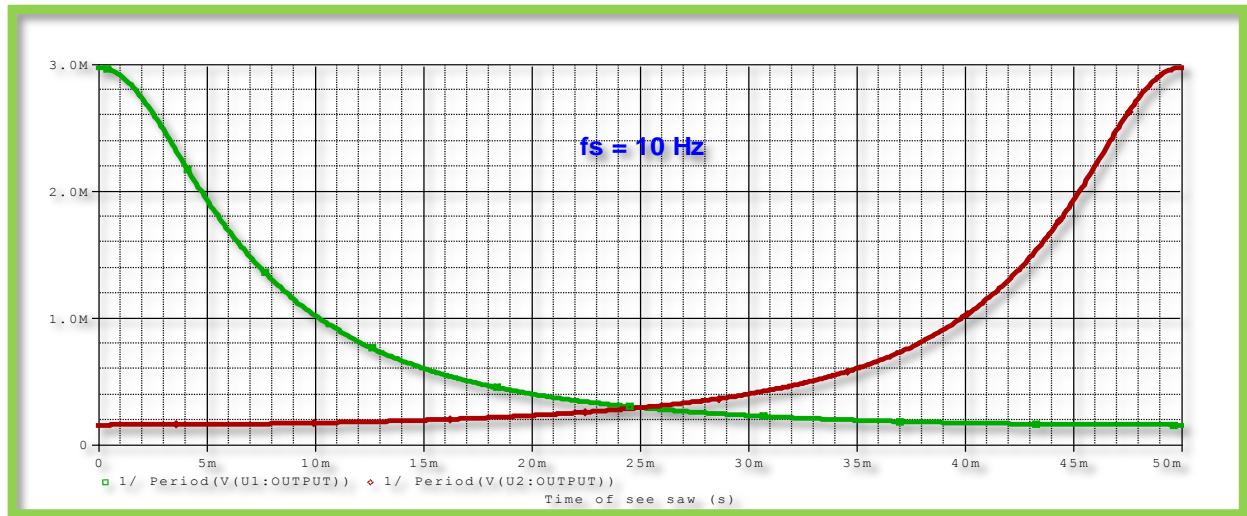
(a)

(b)

(c)

Figure 10 (a-d): Simulation values for different harmonics in the see-saw.

Table 1. Simulation details of frequency hysteresis.

X	delta f1	delta f2	delta f
0.001	0.109400729	8958.646289	4479.3778
0.002	1692127.847	18912.4638	855520.16
0.003	2257759.167	30037.02729	1143898.1
0.004	2540873.66	42551.79359	1291712.7
0.005	2710838.104	56734.72486	1383786.4
0.006	2824187.656	72943.17702	1448565.4
0.007	2905171.185	91644.4259	1498407.8
0.008	2965919.533	113461.451	1539690.5
0.009	3013174.592	139243.6828	1576209.1
0.01	3050982.636	170180.1802	1610581.4
0.011	3081919.134	207988.2244	1644953.7
0.012	3107701.365	255243.2833	1681472.3
0.013	3129518.39	315991.6318	1722755
0.014	3148219.639	396975.1606	1772597.4
0.015	3164428.091	510324.7128	1837376.4
0.016	3178611.023	680289.1565	1929450.1
0.017	3191125.789	963403.6494	2077264.7
0.018	3202250.353	1529034.969	2365642.7
0.019	3212204.17	3221162.707	3216683.4

converted into frequency output in the processing part of the sensor using a timer circuit. Simulation of the proposed system shows a similar result with that of theoretical derivation. The sea saw bar frequency effect is checked and the limitation for this value. This was found in Equation (16). Finally, this novel design provides a platform for electro-mechanical and servomechanism system deviation in form of oscillation and vibration to be harvested into useful electrical signal by the help of designed differential inductive sensor using both coils transducers as shown in Figure 3. The result obtained appears to be at minimum value of 0.001% of FSO which serve as improvement and introduction frequency hysteresis results in both derivations and in simulations.

Conflict of Interest

The authors have not declared any conflict of interest.

REFERENCES

Ezzat G, Cheng HMM (2011). "High-Sensitivity Inductive Pressure Sensor," IEEE Trans. Instrum. Meas. 60(8).

Edgarcio AB, Caballero WU, Aldonate J (1988). "Inductive Proximity Transducer", IEEE Engineering in Medicine & Biology Society 10th Annual International Conference.

Grover D, Deller JR (1999).'Digital Signal Processing And The Microcontroller, chapter 2, Motorola University Press - Prentice Hall Professional Technical Reference, Upper Saddle River, NJ. pp. 15-20.

Hameed SA, Aboaba A, Khalifa AA, Abdalla OO, Daoud AH, Saeed JI, Mahmoud RA (2012). Framework for enhancement of image guided surgery: Finding area of tumor volume, Aust. J. Basic Appl. Sci. 6(1):9-16. (ISI Cited publication).

Mohammed SS, George AB, Vanajakshi L, Venkatraman J (2012). "A Multiple Inductive Loop Vehicle Detection System for Heterogeneous and Lane-Less Traffic," IEEE Trans. Instrum. Meas. 61(5):1353-1361. http://dx.doi.org/10.1109/TIM.2011.2175037

Mohan NM, Shet AR, Kedarnath S, Kumar VJ (2008). "Digital Converter for Differential Capacitive Sensors," IEEE Trans. Instrum. Meas. 57(11):2576-2581. http://dx.doi.org/10.1109/TIM.2008.922109

Mohan NM, George AB, Kumar VJ (2009). "Analysis of a Sigma–Delta Resistance-to-Digital Converter for Differential Resistive Sensors," IEEE Trans. Instrum. Meas. 58(5):1617-1622. http://dx.doi.org/10.1109/TIM.2009.2012949

Ravindra W (2006). 'Inductive Fiber-Meshed Strain and Displacement Transducers for Respiratory Measuring Systems and Motion Capturing Systems' IEEE Sensors J. 6(3).

Saxena SC, Sahu C (1994). "Differential Inductive Ratio Transducer with Short-circuiting Ring for Displacement Measurement", IEEE Trans. Instrum. Meas. 43(5). http://dx.doi.org/10.1109/19.328885

Slamwomir T (2007). "Induction Coil Sensors-a review. Institute of Electrical Theory and Measurement", UlKoszykowa 75,00-661 Warsaw, Poland, pp. 31-46.

LM555 Data sheet (2003). Texas Instruments.

Udaya KM, Duleepa JT (2011). "A Bidirectional Inductive Power Interface for Electric Vehicles in V2G Systems," IEEE Trans. Ind. Elect. 58(10): 4789-4796. http://dx.doi.org/10.1109/TIE.2011.2114312

Appendix 1

Inductance of the part containing the core L_1 is given as:

$$L_1 = \frac{\mu_r \mu_0 N_1^2 A}{l-x} \qquad \text{(A-1)}$$

The inductance of the part with no core L_2 is given as:

$$L_2 = \frac{\mu_0 N_2^2 A}{x} \qquad \text{(A-2)}$$

The numbers of turns in the first and second inductors above the total number of the coil under consideration give by

$$N = N_1 + N_2 \qquad \text{(A-3)}$$

And, therefore, we know that

$$\frac{N_2}{N} = \frac{x}{l} N = \frac{Nx}{l}$$

Similarly;

$$N_1 = \frac{N(l-x)}{l} = N\left(1 - \frac{x}{l}\right) \qquad \text{(A-4)}$$

Substituting the values of N_1 and N_2 into equations above:

$$L_1 = \frac{\mu_r \mu_0 N^2 \left(1 - \frac{x}{l}\right)^2 A}{l-x} = \frac{\mu_r \mu_0 N^2 A(l-x)}{l^2} \qquad \text{(A-5)}$$

$$L_2 = \frac{\mu_0 N^2 \left(\frac{x}{l}\right)^2 A}{x} = \frac{\mu_0 N^2 A x}{l^2} \qquad \text{(A-6)}$$

The total inductance is the series sum of the individual inductances L_1 and L_2, given as:

$$L = L_1 + L_2 \qquad \text{(A-7)}$$

International Journal of Physical Sciences

Related Journals Published by Academic Journals

- African Journal of Pure and Applied Chemistry
- Journal of Internet and Information Systems
- Journal of Geology and Mining Research
- Journal of Oceanography and Marine Science
- Journal of Environmental Chemistry and Ecotoxicology
- Journal of Petroleum Technology and Alternative Fuels